Journal of Power Sources 232 (2013) 123–131

Contents lists available at SciVerse ScienceDirect

Journal of Power Sources

journal homepage: www.elsevier.com/locate/jpowsour

Scandia-stabilized zirconia electrolyte with improved interlamellar bonding by high-velocity plasma spraying for high performance solid oxide fuel cells

Shan-Lin Zhang, Cheng-Xin Li*, Chang-Jiu Li, Guan-Jun Yang, Zhi-Hai Han

State Key Laboratory for Mechanical Behavior of Materials, School of Materials Science and Engineering, Xi'an Jiaotong University, Xi'an, Shaanxi 710049, China

HIGHLIGHTS

- ► High-velocity plasma-sprayed ScSZ electrolyte was used directly to SOFC.
- ► In-flight particle diagnostics are employed to select the optimal spray parameters.
- ► ScSZ prepared by SAPS exhibits higher gas tightness than conventional APS.
- ► Electrolyte gas tightness is improved by the increasing of deposition temperature.
- ► Output power density is increased about 70% with the growth of long columnar crystal.

ARTICLE INFO

Article history:
Received 8 July 2012
Received in revised form
6 December 2012
Accepted 23 December 2012
Available online 10 January 2013

Keywords:
SOFCs
Scandia-stabilized zirconia
Plasma spraying
Particle velocity
Deposition temperature

ABSTRACT

A main challenge of conventional atmospheric plasma spraying (APS) in the application for SOFCs is how to fabricate the dense electrolyte which can be used directly. In this study, supersonic atmospheric plasma spraying (SAPS), one of the high-velocity plasma spraying technologies, was used to prepare scandia-stabilized zirconia (ScSZ) electrolyte to enhance the performance of SOFCs by decreasing the porosity and improving the ionic conductivity with the continuous growth of columnar grains across splat interfaces. The temperature and velocity of in-flight ScSZ particles were measured, and the influences of deposition temperature on the microstructure and cell output performance were investigated. Results showed that the as-sprayed ScSZ prepared by SAPS exhibited higher gas tightness than conventional APS by approximately one order of magnitude. With the increase of deposition temperature from 200 °C to 600 °C, the microstructure of ScSZ electrolyte changed from the traditional lamellar structure with limited interface bonding to the long columnar crystal structure, and the maximum output power densities of the cells with 60 μm ScSZ electrolyte prepared by SAPS increased by more than 70% with the increase of deposition temperature from 200 °C to 600 °C and reached 995 mW cm^{-2} at 1000 °C.

1. Introduction

Solid oxide fuel cells (SOFCs) have been widely investigated as an efficient and environmentally friendly alternative to conventional power generation using fossil fuels. The performance of SOFCs is generally limited by the internal ohmic losses and the electrochemical-catalytic activity of electrodes [1]. Electrolytes have the lowest electrical conductivity among all functional layers in SOFCs, especially at low temperature [2,3]. Therefore, the use of an electrolyte with high electrical conductivity is one of the effective approaches to improve the performance of SOFCs. Scandia-stabilized zirconia (ScSZ) is one of the zirconia-based electrolyte materials that exhibit higher electrical conductivity than other zirconia-based materials. The maximum electrical conductivity of ScSZ bulk is approximately 0.36 S cm^{-1} at 1000 °C, in comparison to 0.16 S cm^{-1} of yttria-stabilized zirconia (YSZ), which has been extensively used in SOFCs [4]. Moreover, ScSZ conductivity at 780 °C is comparable to that of YSZ at 1000 °C [1]. The activation energy for the transport of oxygen ions in the ScSZ materials is also lower than in YSZ materials [1]. Many studies have shown that SOFCs that use ScSZ as electrolytes exhibited better performance than SOFCs using YSZ electrolytes [5,6].

* Corresponding author. Tel.: +86 29 82660970; fax: +86 29 83237910.
E-mail address: licx@mail.xjtu.edu.cn (C.-X. Li).

0378-7753/$ – see front matter © 2013 Elsevier B.V. All rights reserved.
http://dx.doi.org/10.1016/j.jpowsour.2012.12.092

The fabrication process of electrolytes also plays an important role in the SOFC's commercial applications. Atmospheric plasma spraying (APS) is one of the most promising processing methods for the production of the components used in SOFCs; APS has many cost-effective characteristics, including its flexibility and easy automation features, compared with the film-formation processes of electrochemical vapor deposition (EVD) [7], vacuum plasma spraying (VPS) [8], and sol–gel method [9]. Compared with conventional coating technologies, such as tape casting [10], screen printing [11], and dip coating [12], plasma-sprayed electrolyte does not need sintering at a high temperature which will easily introduce many defects, such as warp, crackle and pores for the cells with a large area.

However, the ceramic coatings deposited by traditional APS have high porosity, and the pores in the coating are linked with the unbonded interfaces and microcracks. Because of these features, traditional APS ceramic coating may not be suitable for SOFCs electrolytes, directly [13–17]. Instead, a sintering process, which is described as the "thermal spraying-sintering process", has been investigated following plasma spraying, to obtain improved gas tightness, a thinner layer, and higher electric conductivity of the electrolyte [18,19]. However, the high-temperature sintering process usually causes other problems, including interface reactions, increased cost, and unsuitability for metal-supported SOFCs. Furthermore, the YSZ electrolyte deposited by vacuum plasma spraying (VPS) exhibited acceptable performance [20,21]. Comparing VPS with traditional APS for spraying electrolytes, the main improvements of VPS over APS are a relatively high in-flight particle velocity and temperature obtainable, in addition to the low-pressure atmosphere for deposition. The dense YSZ electrolyte can be fabricated by a three-cathode APS torch, which also showed a relatively high in-flight particle velocity and temperature [22]. Three key parameters influence the coating microstructure and properties: in-flight particle velocity, temperature, and particle size. For the powders with a determined size range, only particle velocity and temperature have strong influences on the coatings microstructure [23]. Many previous investigations showed that the density of the coatings can be significantly improved with the boost of particle velocity when the temperature of particle prior deposition exceeds the melting point. Therefore, a high-velocity thermal spray process is preferable for deposition of dense electrolyte.

As one of the high-velocity plasma spraying technologies, supersonic atmospheric plasma spraying (SAPS) is characterized by high velocity of supersonic plasma jet, which is much higher than that of conventional APS. Furthermore, it works at atmospheric pressure and has operating costs similar to those of traditional APS. Therefore, SAPS will be a potential process for the future fabrication of high performance electrolytes for SOFCs, due to its features of high velocity and temperature.

The gas-leakage channels in the plasma-sprayed ceramic coatings consisted of pores, microcracks, and unbonded interfaces. Although the particle velocity significantly affects the porosity of the coatings, it has limited influence on the cohesive bonding of plasma-sprayed coating [15]. The mean bonding ratio at the interfaces between splats of ceramic coatings deposited by conventional APS or VPS is less than 1/3 of the total apparent interface area; this has a significant influence on ionic conductivity and gas tightness of as-sprayed electrolyte [24].

Recently, another parameter that influences the cohesive bonding of the coatings has been identified [24]: the deposition temperature is the coating surface temperature prior droplet impact during deposition. Our previous research [24] showed that with the increase of deposition temperature, the microstructure of YSZ coatings deposited by APS changed from the typical lamellar structure to the continuous columnar crystal structure. This structural change led to the increased lamellar interface bonding and, subsequently, the increased ionic conductivity of the plasma-sprayed YSZ. Therefore, the electrolyte prepared at a high deposition temperature may exhibit improved performance, with high ionic conductivity and gas tightness.

The purpose of this study was to fabricate a dense electrolyte that can be used directly for SOFCs by high-velocity plasma spraying. The performance of as-sprayed electrolyte would be improved by three aspects. Firstly, ScSZ with a high ionic conductivity was used as the electrolyte material. Then, the ScSZ electrolyte was prepared by SAPS to increase the density and the gas tightness due to the high in-flight particle velocity and temperature. Finally, the ScSZ electrolyte was further improved by the growth of long columnar crystal structures at a relatively high deposition temperature. Therefore, in this study, the ScSZ electrolyte was deposited at different temperatures by SAPS to examine the effect of the deposition temperature on microstructure and gas-leakage rate of ScSZ deposit and SOFC performance. The influences of spray distance on the ScSZ particle velocity and temperature were investigated to examine the factors that control cell performance.

2. Experimental

2.1. Material feedstock

In this study, a fuse-crushed 10 mol% Sc_2O_3-stabilized ZrO_2 doped with 1 mol% CeO_2 and 0.1 mol% Al_2O_3 powder (Fujimi Co., Japan) was used as the electrolyte feedstock. By the addition of CeO_2 [25] and $A1_2O_3$ [26], the 10 mol% Sc_2O_3-stabilized ZrO_2 showed a cubic phase at room temperature and had no phase transformation with the increase of temperature. The powder has a size range of 5–25 μm and shows an irregular shape (Fig. 1a). Commercially available 8 mol% YSZ powder (Fujimi Co., Japan, $-25 + 5$ μm) was also used for comparison to ScSZ. Results from our previous study [27] suggested that plasma-sprayed anode with NiO/YSZ agglomerated powders had a long three-phase boundary (TPB) and exhibited a good performance. Therefore, in order to prepare an anode with sufficient TPB and high electron and ionic conductivity, the agglomerates of NiO particles less than 5 μm with ScSZ particles less than 10 μm were used as the feedstock powders to deposit the anode. The agglomerated powders had a particle size of 50–70 μm (Fig. 1b). In this study, plasma-sprayed $La_{0.8}Sr_{0.2}MnO_3$ (LSM) was used as the cathode. Although the LSM showed relatively low catalytic activity for oxygen reduction at the lower temperatures, it had good chemical and physical compatibility with zirconia-based electrolyte material even at 1000 °C [1]. Therefore, we used commercially available agglomerated LSM powders with a size range of 30–70 μm (Fig. 1c) for the preparation of the cathode to investigate the cells performance.

2.2. In-flight particle diagnostics

The surface temperature and velocity of in-flight ScSZ particles were measured by the spray watch system (spray watch-2i CCD system, Oseir, Finland). In this study, experiments were carried out using a SAPS system (HEPJ-100, 80 kW class) and APS system (GPD-80, Jiujiang, 80 kW class). The anode nozzle of the SAPS torch was designed as a Laval nozzle, which had a throat diameter of 4 mm and exit diameter of 5.5 mm. The spray distance was increased from 70 mm to 140 mm for the SAPS and from 60 mm to 110 mm for the APS to investigate the temperature and velocity of in-flight ScSZ particles (Table 1). An optimal spray distance, in which the particles had a higher temperature and velocity, was selected to fabricate the electrolyte.

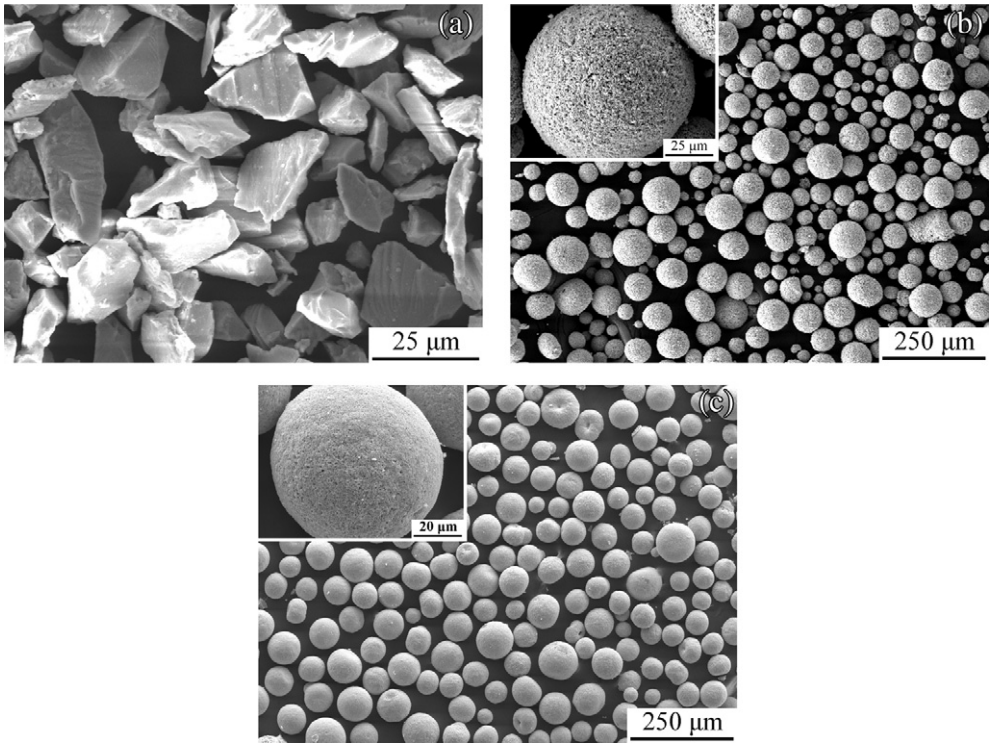

Fig. 1. SEM morphologies of material feedstock: (a) SzSZ powders for electrolyte; (b) NiO/ScSZ agglomerated powders for anode; (c) LSM powders for cathode.

2.3. Cell fabrication

The single cell was supported by the porous Ni50Cr50-Al_2O_3 cermet, deposited by flame spraying with a thickness of 0.8 mm and a diameter of 22 mm [28]. APS (GPD-80, Jiujiang) was used to deposit the anode layer of 55–65 μm on the support with the NiO/ScSZ agglomerated powders at a plasma arc power of 36 kW. The pressures of primary gas Ar and secondary gas H_2 were fixed at 0.8 and 0.4 MPa, respectively. The flow rates of Ar and H_2 were set to 45 and 4.5 L min^{-1}, respectively. The spray distance during deposition was 100 mm. The ScSZ and YSZ electrolytes were deposited by SAPS at deposition temperatures of 200 °C, 400 °C, and 600 °C. The substrate (combined with support and anode) was heated by a flame torch, and the temperature was monitored using a pyrometer (RAYRPM30L3U, Raytek, USA). The spray parameters are shown in Table 1.

Based on the diagnostic results of particles' temperature and velocity, a spray distance of 100 mm was selected. The thickness of electrolytes was controlled at a range of 55–65 μm. The LSM cathode layers were deposited on an area of 0.5 cm^2 with a thickness of 20–30 μm by APS (GPD-80, Jiujiang) at a plasma arc power of 30 kW. The pressures of primary gas Ar and secondary gas H_2 were fixed at 0.8 and 0.4 MPa, respectively. The flow rates of Ar and H_2 were set to 60 and 1.6 L min^{-1}, respectively. The spray distance during spraying maintained at 100 mm. For comparison, the ScSZ electrolyte was also deposited by APS with the spray parameters shown in Table 1 to investigate the effects of particle velocity on the porosity and gas tightness of as-sprayed electrolyte. For each deposition temperature, six cells were prepared to investigate electrolyte performance.

Table 1
Plasma spray parameters for the electrolyte.

Parameter	Unit	SAPS (Value)	APS (Value)
Plasma arc power	kW	72	42
Plasma arc voltage	V	171	60
Plasma arc current	A	420	700
Flow rate of primary gas (Ar)	slpm	65	45
Flow rate of secondary gas (H_2)	slpm	25	7
Powder feed rate	g min^{-1}	25	25
Spray distance	mm	70–140	60–110
Deposition temperature	°C	200, 400, 600	600

2.4. Characterizations of the cell

Before the fabrication of LSM cathode, the gas tightness of the electrolytes was tested after the NiO in the anode was reduced in H_2 atmosphere at 700 °C for 2 h. The sample was connected to a vacuum chamber with a pressure gauge and pumped down to a vacuum condition. The gas permeability across the sample was estimated from the relationship between the pressure difference across the samples and leakage time. The detailed description of the principle and method can be found elsewhere [14,29]. The performance of the single cell was tested in a furnace with a heating and cooling rate of 3 °C min^{-1}. In this study, H_2 as a fuel was bubbled through water maintained at about 30 °C. The output performance of the cells (I–V and I–P curves) was measured in a temperature range of 700–1000 °C under a H_2 flow of 0.1 slpm and O_2 flow of 0.15 slpm. The surface morphology and microstructure of the electrolyte layers were characterized by scanning electron microscopy (SEM, VEGA II-XMU, TESCAN, Czech). The porosity of ScSZ deposits was estimated by analyzing images of cross-sectional microstructures.

3. Results and discussion

3.1. Influences of spray distance on the in-flight ScSZ particle velocity and temperature

The particles' velocity and temperature increased with the increase of spray distance to a maximum value and then decreased

with the further increase of spray distance (Fig. 2a and b); this pattern is generally recognized during plasma spraying [30]. However, the maximum particle velocities reached in APS and SAPS were significantly different. The velocity of ScSZ particles reached a maximum value of 500 m s^{-1} at a spray distance of 100 mm in SAPS, while the maximum velocity of ScSZ particles in APS only reached a maximum velocity of 348 m s^{-1}, a value that is comparable to those reported in other studies [31].

Furthermore, the mean temperature of ScSZ particles in SAPS was significantly higher than in APS under the conditions of the present study. The in-flight particle temperatures at the spray distances of 100 mm and 120 mm reached 3130 °C and 3190 °C, which are higher than the melting point of ScSZ powder (2730 °C). Since a higher in-flight particle velocity and temperature will be beneficial to obtaining denser deposits, ScSZ electrolyte was deposited at an optimized spray distance of 100 mm for SAPS.

After the powder was injected into the plasma jet, there was a process of heating and acceleration for the powder before the velocity and temperature reached their highest values. As a result, the heating process and acceleration process were not completely synchronous; velocity and temperature usually reached peak values at different spray distances. Therefore, it can be concluded that 100 mm was an optimized spray distance for SAPS in the process adopted in this study, and 80 mm may be the best spray distance for APS under this study's parameters (Table 1). Many processing parameters during the spraying process (such as arc current and primary and secondary plasma gas flow rates) had significant influences on the in-flight particle characteristics [32]. The particle velocity of SAPS at a spray distance of 100 mm (500 m s^{-1}) was 44% higher than the particle velocity of APS at a spray distance of 80 mm (348 m s^{-1}; Fig. 2a and b). Moreover, the particle surface temperature of SAPS at 100 mm was also about 400 °C higher than that of APS at 80 mm. This was attributed to the higher flow rates of primary gas (Ar) and secondary gas (H_2), the higher power [31,33,34], and the special structure of the spray gun for SAPS.

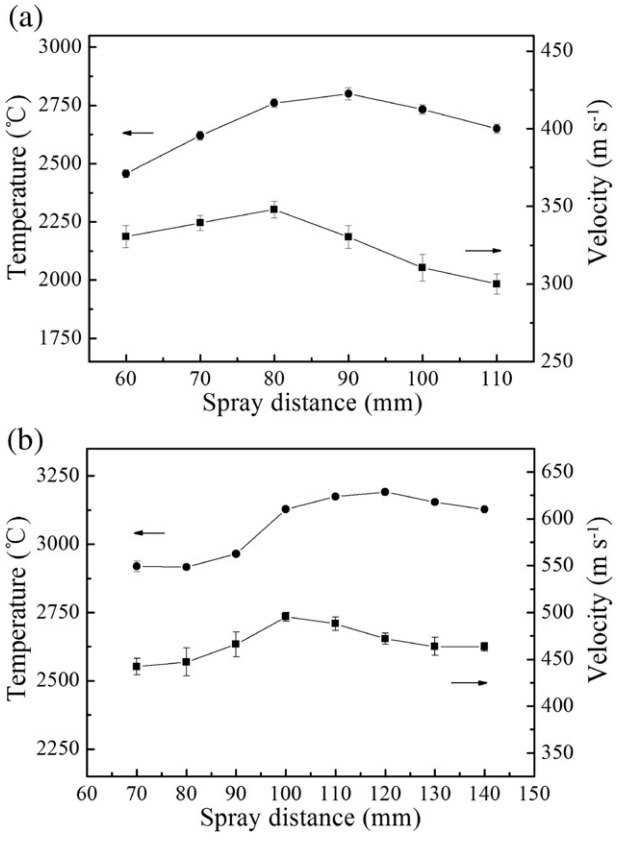

Fig. 2. Effect of spray distance on the velocity and surface temperature of ScSZ particles: (a) for APS; (b) for SAPS.

3.2. Microstructure of plasma-sprayed ScSZ electrolytes

On the porous Ni50Cr50-Al_2O_3 cermet support, the Ni–ScSZ anode, ScSZ electrolyte, and LSM cathode were layered one-by-one in sequence (Fig. 3a). The ScSZ electrolytes exhibited a characteristic microstructure for APS and SAPS at a deposition temperature of 600 °C, indicating the influences of particle velocity and temperature on the electrolyte microstructure (Fig. 3b and c). The pores present in the ScSZ electrolyte prepared by SAPS were much less and smaller, compared with APS ScSZ. The ScSZ electrolytes deposited by APS and SAPS at a deposition temperature of 600 °C had porosities of 6.3 ± 1.4% and 2.6 ± 0.3%, respectively. The low porosity of SAPS ScSZ can be attributed to its high particle temperature and velocity; the high velocity of particles means high kinetic energy, which makes the molten particle easily fill the cavities of a rough surface upon impact. Moreover, the wettability of molten particle can be also enhanced by the increase of temperature [35].

To reveal the influences of deposition temperature on the interlamellar bonding between ScSZ splats, the ScSZ deposits were fractured, since no useful lamellar details can be obtained from normal metallographic samples. The microstructure of ScSZ deposits changed from the typical lamellar structure with limited lamellar bonding (Fig. 4a) to the continuous columnar crystal structure (Fig. 4b and c) with the increase of deposition temperature. The columnar crystals grew within a splat, and the length of columnar crystals was comparable to a splat thickness of about 1 μm at a deposition temperature of 200 °C (Fig. 4a). In addition, unbonded interfaces between lamellae were present in the deposit, and microcracks were present in individual splats. When the substrate was preheated to 400 °C, the typical columnar crystals grew continuously over several lamellae and had a length of about 4–5 μm (Fig. 4b). In addition, when the deposition temperature reached 600 °C, long columnar crystals more than 10 μm with fewer unbonded interfaces and microcracks were present in the ScSZ deposit (Fig. 4c). This indicates that the effective bonding was formed through several lamellae. Such long columnar grains were formed by the growth of the grains of solidifying liquid splat through heterogeneous nucleation on the previously deposited splats. These results were consistent with previous results for plasma-sprayed YSZ coatings at high preheating temperatures [36].

Although other studies [23,31] showed that it was possible to achieve a dense ceramic deposit by plasma spraying with a high particle velocity and temperature, a previous investigation demonstrated difficulties in increasing the lamellar bonding ratio over one-third between lamella in the ceramic coating deposited following the conventional coating deposition routine [13,15,16]. The ScSZs deposited by SAPS with a deposition temperature of 200 °C in this study also showed a typical lamellar structure (Fig. 4a), although the in-flight particle reached a velocity of about 500 m s^{-1}, which was even higher than that obtained with the VPS process [8,37].

In addition, the surface morphologies of SAPS ScSZ differed among different deposition temperatures (Fig. 5). Many microcracks were found from the surface of the ScSZ deposited at 200 °C (Fig. 5a). However, with the increase of deposition temperature (Fig. 5b and c), it becomes difficult to find the microcracks from the coating surface. This could be attributed to a lower quenching stress evolved during rapid solidification of molten droplets on a higher

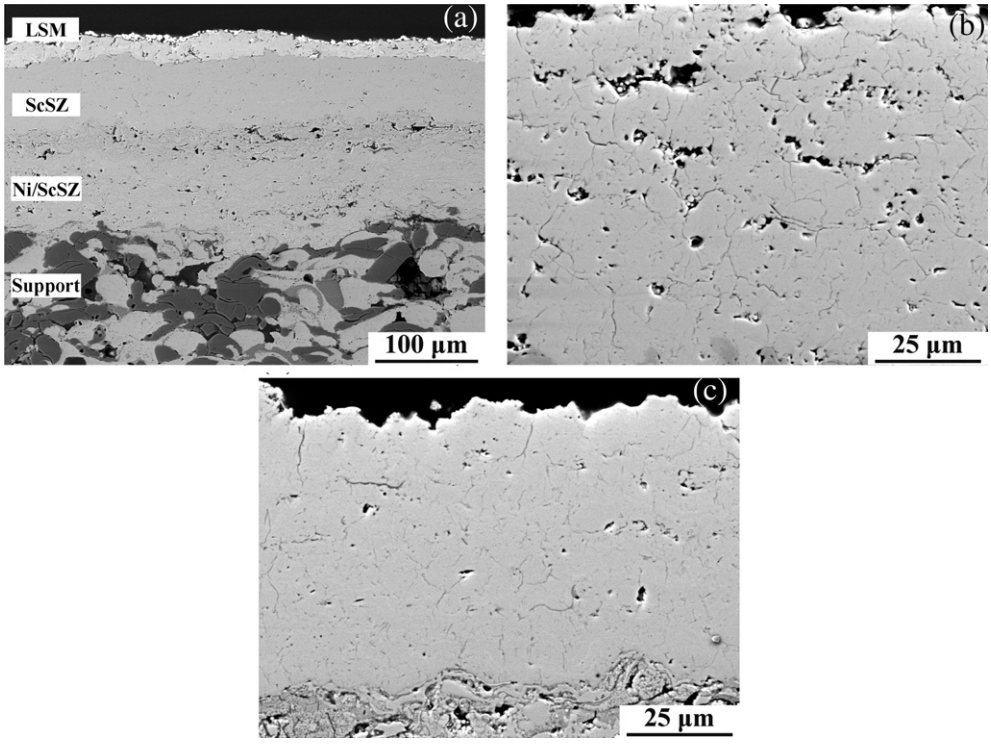

Fig. 3. Microstructure of the polished cross-section of single cell and ScSZ electrolytes: (a) cermet-supported single cell; (b) ScSZ electrolyte deposited at 600 °C by APS; (c) ScSZ electrolyte deposited at 600 °C by SAPS.

deposition temperature, which decreased the thermal gradient between the substrate and splats. The limited microcracks in ScSZ deposited at high deposition temperature further lowered the porosity.

3.3. Gas tightness of the ScSZ electrolytes

Pores in the ScSZ deposits (Figs. 3 and 4) will decrease their ionic conductivity. However, only interconnected pores in the electrolyte

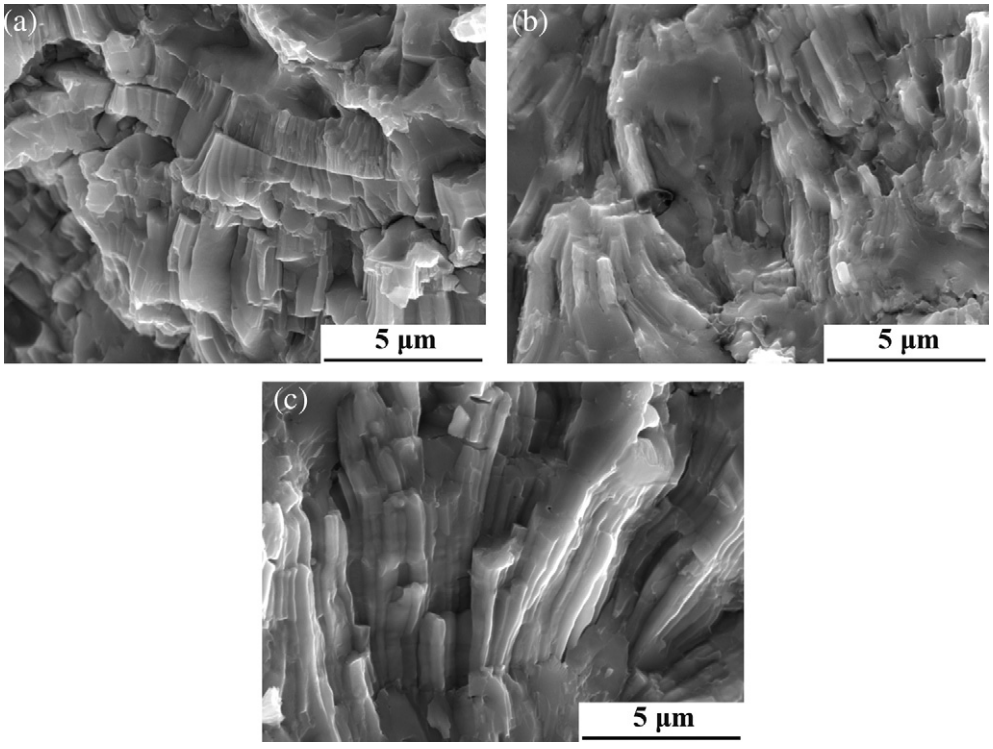

Fig. 4. Microstructure of the fractured ScSZ electrolytes deposited by SAPS at difference deposition temperatures: (a) 200 °C; (b) 400 °C; (c) 600 °C.

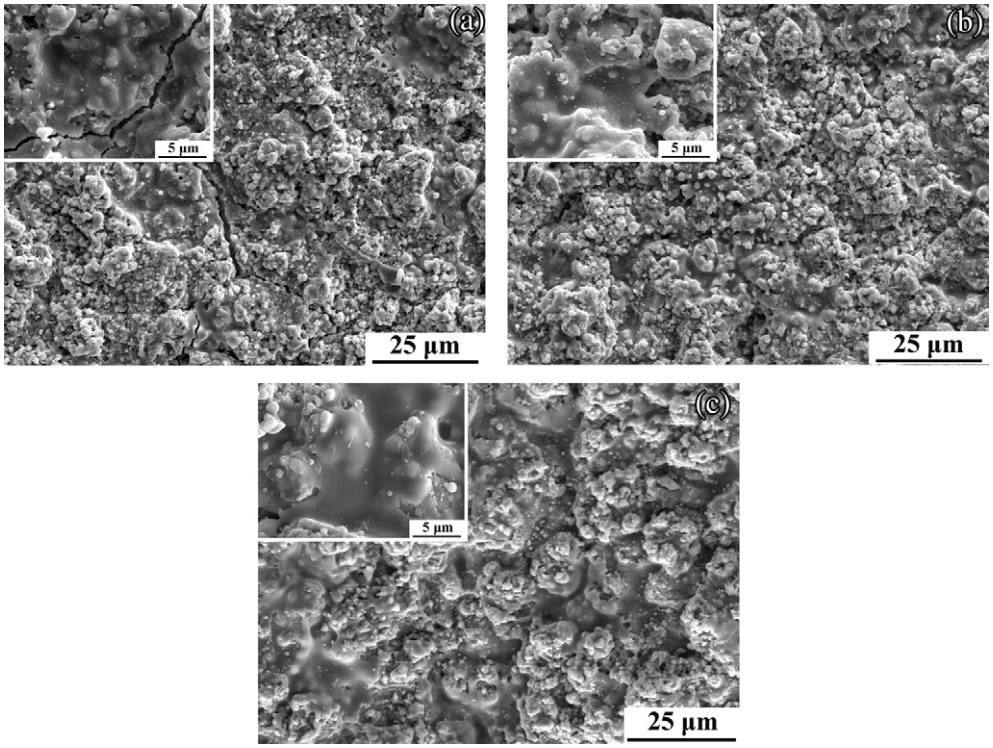

Fig. 5. Surface morphologies of the ScSZ electrolytes deposited by SAPS at difference deposition temperatures: (a) 200 °C; (b) 400 °C; (c) 600 °C.

will lead to leakage of fuel or oxidizing gas under the operation of the cells. Fig. 6a shows the change of the pressure difference across the cells assembled with ScSZ deposits, and Fig. 6b shows the gas-leakage rate through ScSZ deposits. The gas tightness was significantly improved by the increase of deposition temperature from the time–ΔP curves (Fig. 6a). The ScSZ fabricated by SAPS at a deposition temperature of 200 °C showed a specific gas-leakage rate of 3.5×10^{-7} cm^4 gf^{-1} s^{-1}, and it decreased to 7×10^{-8} cm^4 gf^{-1} s^{-1} when the deposition temperature was increased to 600 °C. In comparison, the ScSZ fabricated by APS at a deposition temperature of 600 °C exhibited a specific gas-leakage rate of 7.2×10^{-7} cm^4 gf^{-1} s^{-1} in this study. Compared with the ScSZ fabricated by SAPS at a deposition temperature of 200 °C, the gas-leakage rate of the ScSZ electrolyte deposited at 600 °C decreased by nearly one order of magnitude. This result can be attributed to the decrease of unbonded interfaces among splats and microcracks in individual splats, which cut off the pathway for gas leakage.

Our previous study [38] reported that the gas-leakage rate of the as-sprayed YSZ deposited by APS in a conventional routine was 1.02×10^{-6} cm^4 gf^{-1} s^{-1}. Compared with these data, the leakage rate of 3.5×10^{-7} cm^4 gf^{-1} s^{-1} obtained for the ScSZ fabricated by SAPS with the same deposition temperature of about 200 °C in this study was one order of magnitude lower. The same result was also obtained from the ScSZs fabricated by SAPS and APS at a deposition temperature of 600 °C in the present study.

The velocity of in-flight particles can also be increased by using VPS, compared with APS. Tsukuda et al. [39] reported that the gas permeability of the YSZ coating deposited by VPS was lower in value by one order of magnitude, compared to that of the coating deposited by APS. For the plasma-sprayed ceramic coatings by APS or VPS, the main difference was the velocity of in-flight particles, since changes of atmospheric pressure from APS to VPS and gas atmosphere influenced little splat structure. However, the thickness of splat will decrease with the increase of the velocity of in-flight particles [40]. For the same thickness of deposit, more splats were needed in the direction perpendicular to the deposit surface when the velocity of spray droplet was high; as a result, the length of the gas-leakage pathway increased. Moreover, high velocity also contributed to the decrease of gaps within unbonded interface areas.

3.4. Cell performance

The open circuit voltage (OCV) changed with test temperature of the cells for ScSZ electrolyte deposited at different deposition temperatures by SAPS is shown in Fig. 7. The OCV of the cells increased with the increase of deposition temperature at all of the operation temperatures. The maximum OCV of the cell deposited at 200 °C was 0.93 V, and it increased to 1.04 V when the deposition temperature was increased to 600 °C. In comparison, at an operation temperature of 800 °C, the cell deposited at 600 °C had an OCV of 1.01 V. This value was lower than the theoretical voltage [1], meaning that the electrolyte was not dense enough. However, it is an acceptable value for SOFCs operation. In addition, the thickness of ScSZ electrolyte in the present study was about 60 μm, and the OCV at 1000 °C reached to 0.96 V, which is also an acceptable value for SOFC operation. Tsukuda et al. [39] reported the performance of a 10-kW class SOFC module. In their module, YSZ electrolyte of about 100 μm thickness deposited by VPS exhibited an OCV of about 1 V at 1000 °C. The gas-leakage rate of plasma-sprayed ceramic deposit will be significantly increased with the reduction of deposit thickness, especially when the thickness of deposit is lower than 200 μm [41]. Therefore, it can be concluded that the OCV of ScSZ electrolyte fabricated by SAPS at a high deposition temperature was comparable to that for the cell by VPS electrolyte, which has found practical application in a SOFC module displaying long-term operation up to 2000 h [39]. Therefore, the as-sprayed SAPS ScSZ at a high deposition temperature should be applicable as the electrolyte of SOFCs.

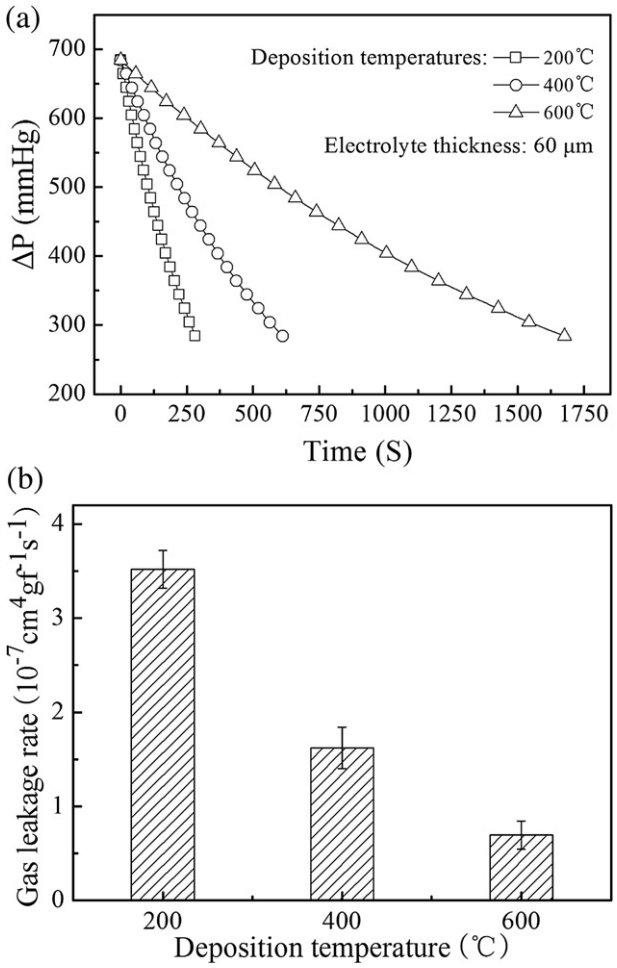

Fig. 6. Gas tight property of the ScSZ electrolytes prepared by SAPS at different deposition temperatures: (a) change of the pressure difference across the cells assembled with ScSZ deposits; (b) gas-leakage rate at different deposition temperatures.

The output performances of the cells with as-sprayed ScSZ electrolyte are shown in Fig. 8. The cell voltage decreased nearly linearly with the increase of current density when the operation temperature was above 800 °C. These results mean that the ohmic polarization is mainly responsible for the reduction of cell voltage at a high current density. However, the activation polarization can

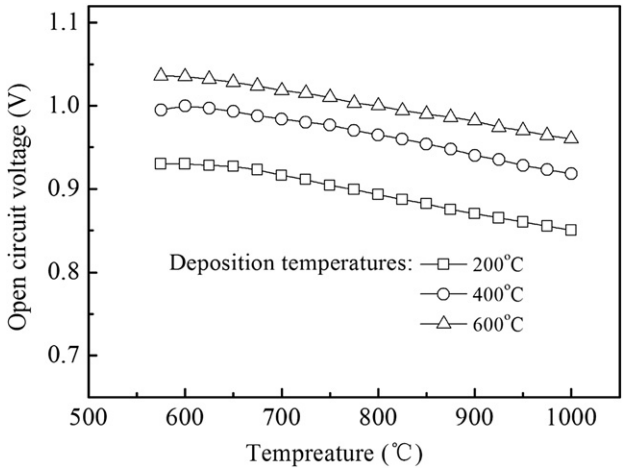

Fig. 7. Open circuit voltage of the cells fabricated with ScSZ electrolyte by SAPS.

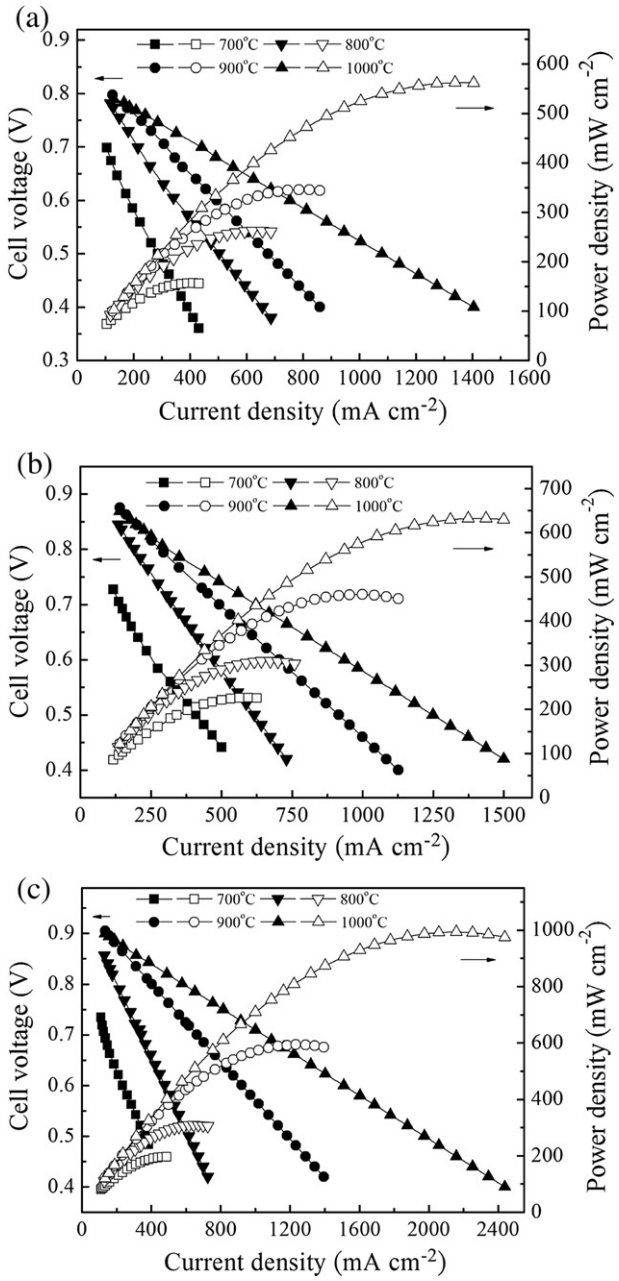

Fig. 8. Output performance of as-sprayed cells fabricated with ScSZ electrolyte at different deposition temperatures: (a) 200 °C; (b) 400 °C; (c) 600 °C.

be observed at the current density lower than 200 mA cm^{-2} at 700 °C because of the low catalytic activity of the LSM cathode at low temperature. At an operating temperature of 800 °C, the cells showed the power densities at a cell voltage of 0.7 V of about 150, 210, and 250 mW cm^{-2} at the deposition temperatures of 200 °C, 400 °C and 600 °C, respectively. The previous investigation on the effect of conventional plasma-sprayed ScSZ thickness on SOFC output performance showed that the maximum output power was increased nearly by a factor of two at 800 °C when ScSZ thickness was reduced from 60 μm to 40 μm [6]. Taking account of the low electrochemical-catalytic activity of present LSM cathode at low temperature, the performance of the present SAPS ScSZ at low temperature is acceptable when it is compared with electrolyte deposited by other high-velocity plasma spray process as that reported by Hathiramani et al. [22].

When the cells were tested at 900 °C and 1000 °C, the cell performance was significantly improved with the increase of operating temperature. Moreover, the deposition temperature also had a great influence on the output performance. At the deposition temperature of 600 °C and a cell voltage of 0.7 V, the power densities reached about 464 and 754 mW cm^{-2} at the operating temperatures of 900 °C and 1000 °C, respectively. In addition, at 1000 °C, when the deposition temperature was increased from 200 °C to 600 °C, the maximum power density increased about 77%, reaching 995 mW cm^{-2}.

Since anodes and cathodes of the cells were prepared by the same process, the present results indicate that the greatest contribution to the enhancement of performance resulted from the increase of conductivity of electrolyte. The ionic conductivity of plasma-sprayed ZrO_2-based electrolyte was influenced by the lamellar bonding, which was significantly affected by the deposition temperature (Fig. 4). The ionic conductivity was improved by the growth of long columnar grains, which increased the interlamellar mean bonding ratio in the deposit. Furthermore, the decrease of porosity also enhanced the ionic conductivity. In our previous study on the plasma-sprayed YSZ coatings [42], the ionic conductivity of APS YSZ was improved by 53% (from 0.036 S cm^{-1} to 0.055 S cm^{-1}) when the mean deposition temperature increased from 167 °C to 686 °C. The cell voltage decreased nearly linearly with the increase of the current density at all deposition temperatures when the cell was operated at 900 °C and 1000 °C (Fig. 8). Because no significant concentration polarization was observed, the decrease of the cells voltage was resulted from both ohmic polarization and electrode polarizations. Therefore, at 1000 °C, the area-specific resistance (ASR) of the present cell can be obtained from the output performance. At 1000 °C, the ASR was 0.62, 0.33, and 0.25 Ω cm^2 at the deposition temperature of 200 °C, 400 °C, and 600 °C, respectively. The ASR decreased about 60% when the deposition temperature increased from 200 °C to 600 °C. Since the cells had the same electrodes, it can be concluded that the conductivity of SAPS ScSZ electrolyte at 1000 °C increased more than 60% with the increase of deposition temperature from 200 °C to 600 °C. The long columnar grains at high deposition temperature allow the oxygen ions to transfer directly across the interface and significantly reduce the resistance. As a result, the ionic conductivity of the ScSZ deposit layer increased significantly, and the cell performance improved greatly.

In addition, the maximum output power densities of the cells assembled with SAPS ScSZ and SAPS YSZ tested at different temperatures are shown in Table 2. The maximum power density increased when the electrolyte changed from YSZ to ScSZ. The maximum power density increased by 35%, 43%, and 66% at the operation temperatures of 800 °C, 900 °C, and 1000 °C, respectively. The increase of power density at low operation temperature was not as high as expected from the change of electrolyte material and operation temperature. Since both anodes and cathodes of two types of cells were prepared by the same process, this result could be attributed to the fact that the electrode polarization influenced the performance of cells more than ohmic polarization did, especially at the low operation temperature and the high-conductivity electrolyte. This result is consistent with our previous study [6] and also indicates that the SAPS ScSZ electrolyte deposited at a high temperature has great potential in the application for the intermediate-temperature SOFC.

Table 2
The maximum power densities (mW cm^{-2}) of the cell using YSZ and ScSZ electrolyte deposited by SAPS at a deposition temperature of 600 °C tested at different temperatures.

Electrolyte material	800 °C	900 °C	1000 °C
YSZ	229	416	600
ScSZ	310	594	995

4. Conclusions

ScSZ electrolytes were prepared by high-velocity plasma spraying at different deposition temperatures up to 600 °C. Compared with the ScSZ fabricated by APS, the porosity of the ScSZ fabricated by SAPS at a deposition temperature of 600 °C decreased about 60%. In addition, with the increase of deposition temperature, the ScSZ electrolyte changed from the conventional lamellar structure to the long columnar crystal structure. Results showed that the interlamellar bonding in the ScSZ deposit significantly improved with the increase of deposition temperature. The gas tightness of ScSZ was enhanced by the improvement of microstructure. As a result of the change in the electrolyte structure, the performance of the cell assembled with the as-sprayed ScSZ was enhanced. When the deposition temperature increased from 200 °C to 600 °C, the maximum power density increased by more than 70% and reached 995 mW cm^{-2} at 1000 °C. Moreover, the power density of the cell increased by 66% at 1000 °C when the electrolyte was changed from YSZ to ScSZ. These results demonstrate the potential applicability of SAPS ScSZ electrolyte deposited at a high temperature to be used in SOFC directly.

Acknowledgments

This research was supported by the National Natural Science Foundations of China (Grant Nos. 50725101, 51072161)

References

[1] S.C. Singhal, K. Kendall, High Temperature Solid Oxide Fuel Cells: Fundamentals, Design and Application, Elsevier, 2004.
[2] S.J. Geng, J.H. Zhu, Z.G. Lu, Scripta Mater. 55 (2006) 239–242.
[3] K.J. Yoon, P. Zink, S. Gopalan, U.B. Pal, J. Power Sourc. 172 (2007) 39–49.
[4] Y. Arachi, H. Sakai, O. Yamamoto, Y. Takeda, N. Imanishai, Solid State Ionics 121 (1999) 133–139.
[5] Z. Cai, T.N. Lan, S. Wang, M. Dokiya, Solid State Ionics 152–153 (2002) 583–590.
[6] C.J. Li, C.X. Li, H.G. Long, Y.Z. Xing, G.J. Yang, Solid State Ionics 179 (2008) 1575–1578.
[7] M. Inaba, A. Mineshige, T. Maeda, S. Nakanishi, T. Ioroi, T. Takahashi, A. Tasaka, K. Kikuchi, Z. Ogumi, Solid State Ionics 104 (1997) 303–310.
[8] M. Lang, R. Henne, S. Schaper, G. Schiller, J. Therm. Spray Technol. 10 (2001) 618–625.
[9] S.G. Kim, S.P. Yooh, S.W. Nam, S.H. Hyun, S.A. Hong, J. Power Sourc. 110 (2002) 222–228.
[10] S. Le, K.N. Sun, N. Zhang, X. Zhu, H. Sun, Y.X. Yuan, X. Zhou, J. Power Sourc. 195 (2010) 2644–2648.
[11] X. Ge, X. Huang, Y. Zhang, Z. Lu, J. Xu, K. Chen, D. Dong, Z. Liu, J. Miao, W. Su, J. Power Sourc. 159 (2006) 1048–1050.
[12] H. Tikkanen, C. Suciu, I. Wærnhus, A.C. Hoffmann, J. Eur. Ceram. Soc. 31 (2011) 1733–1739.
[13] A. Ohmori, C.J. Li, Thin Solid Films 201 (1991) 241–252.
[14] C.J. Li, X.J. Ning, C.X. Li, Surf. Coat. Technol. 190 (2005) 60–64.
[15] A. Ohmori, C.J. Li, Y. Arata, Trans. Jpn. Weld. Res. Inst. 19 (1990) 259–270.
[16] C.J. Li, A. Ohmori, Surf. Coat. Technol. 82 (1996) 254–258.
[17] C.J. Li, C.X. Li, Y.Z. Xing, M. Gao, G.J. Yang, Solid State Ionics 177 (2006) 2065–2069.
[18] K. Okumura, Y. Aihara, S. Ito, S. Kawasaki, J. Therm. Spray Technol. 9 (2000) 354–359.
[19] K.A. Khor, X.J. Chen, S.H. Chan, L.G. Yu, Mater. Sci. Eng. A 366 (2004) 120–126.
[20] C. Zhang, H.L. Liao, C.J. Li, C.X. Li, W.Y. Li, G. Zhang, C. Coddet, X.J. Ning, J. Therm. Spray Technol. 15 (2006) 598–603.
[21] A.A. Syed, Z. Ilhan, J. Arnold, G. Schiller, H. Weckmann, J. Therm. Spray Technol. 15 (2006) 617–622.
[22] D. Stöver, D. Hathiramani, R. Vaßen, R.J. Damani, Surf. Coat. Technol. 201 (2006) 2002–2005.
[23] R. McPherson, Surf. Coat. Technol. 39-40 (1989) 173–181.
[24] Y.Z. Xing, C.J. Li, C.X. Li, G.J. Yang, J. Power Sourc. 176 (2008) 31–38.
[25] Y. Arachi, T. Asai, O. Yamamoto, Y. Takeda, N. Imanishi, K. Kawate, J. Electrochem. Soc. 148 (2001) A520–A523.
[26] C. Varanasi, C. Juneja, C. Chen, B. Kumar, J. Power Sourc. 147 (2005) 128–135.

[27] C.X. Li, C.J. Li, L.J. Guo, Int. J. Hydrogen Energy 35 (2010) 2964–2969.
[28] S.L. Zhang, C.X. Li, C.J. Li, G.J. Yang, J. Therm. Spray Technol. (2012). http://dx.doi.org/10.1007/s11666-012-9868-5.
[29] A.E. Scheidegger, The Physics of Flow Through Porous Media, third ed., University of Toronto Press, Toronto, 1974, pp. 73–97.
[30] A. Vardelle, M. Vardelle, P. Fauchais, Plasma Chem. Plasma Process. 2 (1982) 255–291.
[31] C. Zhang, C.J. Li, H.L. Liao, M.P. Planche, C.X. Li, C. Coddet, Surf. Coat. Technol. 202 (2008) 2654–2660.
[32] S. Guessasma, G. Montavon, C. Coddet, Surf. Coat. Technol. 192 (2005) 70–76.
[33] M. Cuglietta, O. Kesler, J. Therm. Spray Technol. 21 (2012) 448–460.
[34] C. Zhang, A.F. Kanta, C.X. Li, C.J. Li, M.P. Planche, H.L. Liao, C. Coddet, Surf. Coat. Technol. 204 (2009) 463–469.
[35] N. Sobczak, M. Singh, R. Asthana, Curr. Opin. Colloid. Interface Sci. 9 (2005) 241–253.
[36] Y.Z. Xing, C.J. Li, J.H. Qiao, G.X. Wang, in: International Mechanical Engineering Congress and Exposition, vol. 8, 2007, pp. 1837–1844.
[37] Z. Salhi, S. Guessasma, P. Gougeon, D. Klein, C. Coddet, Aerosp. Sci. Technol. 9 (2005) 203–209.
[38] C.X. Li, C.J. Li, G.J. Yang, J. Therm. Spray Technol. 18 (2009) 83–89.
[39] H. Tsukuda, A. Notomi, N. Hisatome, J. Therm. Spray Technol. 9 (2000) 364–368.
[40] S. Fantassi, M. Vardelle, A. Vardelle, P. Fauchais, J. Therm. Spray Technol. 2 (1993) 379–384.
[41] Y. Arata, A. Ohmori, C.J. Li, Thin Solid Films 156 (1988) 315–325.
[42] Y.Z. Xing, C.J. Li, Q. Zhang, C.X. Li, G.J. Yang, J. Am. Ceram. Soc. 91 (2008) 3931–3936.